HHS Public Access

Author manuscript

Gastroenterology. Author manuscript; available in PMC 2018 April 19.

Published in final edited form as:

Gastroenterology. 2018 March ; 154(4): 1024–1036.e9. doi:10.1053/j.gastro.2017.10.050.

Nanoliposome C6-Ceramide Increases the Anti-tumor Immune Response and Slows Growth of Liver Tumors in Mice

Guangfu Li[1,2,3,*], **Dai Liu**[1,2,*], **Eric T. Kimchi**[1,2], **Jussuf T. Kaifi**[1,2], **Xiaoqiang Qi**[1,2], **Yariswamy Manjunath**[1,2], **Xinjian Liu**[1,2], **Tye Deering**[4], **Diego M. Avella**[1,2], **Todd Fox**[4], **Don C. Rockey**[5], **Todd D. Schell**[6], **Mark Kester**[5], and **Kevin F. Staveley-O'Carroll**[1,2]

[1]Department of Surgery, University of Missouri-Columbia, Columbia, Missouri

[2]Ellis Fischel Cancer Center, University of Missouri-Columbia, Columbia, Missouri

[3]Department of Molecular Microbiology and Immunology, University of Missouri-Columbia, Columbia, Missouri

[4]Department of Pharmacology, University of Virginia, Charlottesville, Virginia

[5]Department of Medicine, Medical University of South Carolina, Charleston, South Carolina

[6]Department of Microbiology and Immunology, Pennsylvania State University College of Medicine, Hershey, Pennsylvania

Abstract

BACKGROUND & AIMS—Ceramide, a sphingolipid metabolite, affects T-cell signaling, induces apoptosis of cancer cells, and slows tumor growth in mice. However, it has not been used as a chemotherapeutic agent because of its cell impermeability and precipitation in aqueous solution. We developed a nanoliposome-loaded C6-ceremide (LipC6) to overcome this limitation and investigated its effects in mice with liver tumors.

METHODS—Immune competent C57BL/6 mice received intraperitoneal injections of carbon tetrachlo-ride and intra-splenic injections of oncogenic hepatocytes. As a result, tumors resembling human hepatocellular carcinomas developed in a fibrotic liver setting. After tumors formed, mice were given an injection of LipC6 or vehicle via tail vein every other day for 2 weeks. This was followed by administration, also via tail vein, of tumor antigen-specific (TAS) $CD8^+$ T

Address requests for reprints to: Kevin F. Staveley-O'Carroll, MD, PhD, Professor, Chair of Surgery, Director of Ellis Fischel Cancer Center, One Hospital Drive, Mc501, University of Missouri-Columbia, Columbia, MO 65212. ocarrollk@health.missouri.edu; fax: 573-884-4585; or Guangfu Li, PhD, DVM, Assistant Professor, Department of Surgery, Molecular Microbiology and Immunology, Ellis Fischel Cancer Center, University of Missouri-Columbia, One Hospital Dr., Medical Sciences Building, M272, Columbia, MO 65212. liguan@health.missouri.edu; fax: 573-884-4585.

Dai Liu's current affiliation is at Vanderbilt University School of Medicine, Nashville, Tennessee.

Conflicts of interest

The authors declare no conflicts.

Competing financial interests

The Penn State Research Foundation has licensed ceramide nanoliposomes and other nonliposomal nanotechnology to Keystone Nano Inc (State College, PA). Dr Mark Kester is the Chief Medical Officer of Keystone Nano Inc.

Supplementary Material

Note: To access the supplementary material accompanying this article, visit the online version of *Gastroenterology* at www.gastrojournal.org, and at https://doi.org/10.1053/j.gastro.2017.10.050.

cells isolated from the spleens of line 416 mice, and subsequent immunization by intraperitoneal injection of tumor antigen-expressing B6/WT-19 cells. Tumor growth was monitored with magnetic resonance imaging. Tumor apoptosis, proliferation, and AKT expression were analyzed using immunohistochemistry and immunoblots. Cytokine production, phenotype, and function of TAS $CD8^+$ T cells and tumor-associated macrophages (TAMs) were studied with flow cytometry, real-time polymerase chain reaction (PCR), and ELISA. Reactive oxygen species (ROS) in TAMs and bone marrow-derived macrophages, induced by colony stimulating factor 2 (GMCSF or CSF2) or colony stimulating factor 1 (MCSF or CSF1), were detected using a luminescent assay.

RESULTS—Injection of LipC6 slowed tumor growth by reducing tumor cell proliferation and phosphorylation of AKT, and increasing tumor cell apoptosis, compared with vehicle. Tumors grew more slowly in mice given the combination of LipC6 injection and TAS $CD8^+$ T cells followed by immunization compared with mice given vehicle, LipC6, the T cells, or immunization alone. LipC6 injection also reduced numbers of TAMs and their production of ROS. LipC6 induced TAMs to differentiate into an M1 phenotype, which reduced immune suppression and increased activity of $CD8^+$ T cells. These results were validated by experiments with bone marrow-derived macrophages induced by GMCSF or MCSF.

CONCLUSIONS—In mice with liver tumors, injection of LipC6 reduces the number of TAMs and the ability of TAMs to suppress the anti-tumor immune response. LipC6 also increases the anti-tumor effects of TAS $CD8^+$ T cells. LipC6 might therefore increase the efficacy of immune therapy in patients with hepatocellular carcinoma.

Graphical Abstract

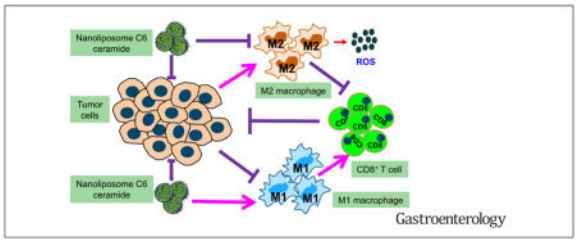

Keywords

HCC Model; Liver Cancer; Nanotechnology; Tumor Microenvironment; Immune Regulation

Hepatocellular cancer (HCC) is now the second leading cause of cancer death with limited therapeutic options.[1] Novel therapies and approaches, therefore, are urgently needed. Manipulating the immune system for the treatment of established cancers has become part of the standard of care for several cancers.[2–4] Studies of immune checkpoints have led to important advances in the development of immunotherapeutic drugs.[5,6] For example, antibody-mediated blockade of cytotoxic T-lymphocyte-associated protein 4 (CTLA-4) and programmed death-1 (PD-1) has been approved by the US Food and Drug Administration for the treatment of advanced melanoma, bladder, head and neck, and lung cancer.[7] These exciting advances in multiple cancer types support the translation of immunotherapies to additional cancers, including HCC.[8] However, no immune-based therapeutic strategy has been successfully translated into an effective treatment for HCC.[9] This failure is partially

explained by the lack of a clinically relevant animal model and the challenge of overcoming tumor-induced immune tolerance in the liver.[10,11]

Ceramide, a sphingolipid metabolite, has been demonstrated to be a powerful tumor suppressor[12–14] and may be involved in immune regulation.[15] Some studies indicate that ceramide is an essential component of T cell receptor (TCR) signaling machinery. Pharmacologic or molecular inhibition of ceramide production impairs TCR-induced interleukin-2 (IL2) production and programmed cell death. Exogenous ceramide administration or sphingomyelinase-induced endogenous ceramide accumulation resulted in reconstitution of both responses.[15] We have demonstrated that ceramide induces p-AKT–dependent apoptosis in human HCC cells in vitro and suppresses their xenograft tumor growth in vivo,[16] exerting an inherent tumoricidal effect. In addition, we recently developed a clinically relevant murine model that mimics immune-tolerant human HCC.[17] Using this model, we are able to test if injection of ceramide can enhance antitumor immunotherapeutic strategies by significantly modulating the profound immunotolerant tumor microenvironment (TME) typical of HCC.

A pro-apoptotic role of ceramide has been widely demonstrated in different cancers, including in HCC,[13,14] Despite its key role in regulating tumor cell growth and death, its cell impermeability and precipitation in aqueous solution have limited ceramide's use as a therapeutic agent. Using nanotechnology advances in drug delivery, we prepared a nanoliposome-loaded C6-ceramide (LipC6) (Supplementary Figure 1).[18] This formulated LipC6 allows C6-ceramide to travel through the bloodstream and target tumor cells through enhanced cellular permeability and retention, facilitating its potential clinical use as a drug.[18,19] Moreover, extensive preclinical toxicology studies, including physiochemical characterization and PK/PD analyses, have been completed for LipC6 in 2 species (rats and beagles).[18] Further, our investigational new drug application for LipC6 was just successfully approved (109471). This 90-nm–sized, −8 mV, 15 molar percent PEG, 30 molar percent C6-ceramide nanoliposome has a shelf life greater than 18 months. We have also published that ceramide is released from LipC6 by intrabilayer movement.[20] Specifically, the C6-ceramide partitions from the nano-platform to cells within the TME, including tumor cells and tumor-associated macrophages (TAMs). Macrophages are key players in the homeostatic function of the liver. In response to changes in the local microenvironment, macrophages undergo polarized activation to M1 or M2.[21] M1 and M2 macrophages display different molecular phenotypes and release different cytokines, suppressing or promoting tumor growth. Reactive oxygen species (ROS) production has been demonstrated to be critical for macrophage differentiation.[22] With our clinically relevant HCC model, we now demonstrate that LipC6 mitigates the profound immunotolerant TME. This undocumented function is associated with modulation of TAMs through ROS signaling. LipC6 inherent tumoricidal effect combining with its ability to activate antitumor immunity results in the eradication of established tumors.

Materials and Methods

Mice

Male C57BL/6 mice were purchased from Jackson Laboratory (Bar Harbor, ME). Line MTD2 transgenic mice that express full-length SV40 T antigen (TAg) driven by the major urinary protein (MUP) promoter have been previously described.[23] Line 416 mice served as the source of TAg-specific $CD8^+$ T cells (TCR-I T cells) were described previously.[24] All experiments with mice were performed under a protocol approved by the Institutional Animal Care and Use Committee. All mice received humane care according to the criteria outlined in the "Guide for the Care and Use of Laboratory Animals."

Peptides, Reagent and Antibodies

Peptides were synthesized in Penn State Hershey Macro-molecular Core Facility (Hershey, PA) and solubilized in dimethyl sulfoxide (DMSO). LipC6 (30 mol% ceramide) and vehicle (no C6-ceramide) were prepared by Dr Mark Kester as described previously.[18] Unlabeled and fluorochrome-conjugated antibodies against CD16/CD32, CD3, CD8a, CD4, CD25, FoxP3, CD11b, F4/80, CD11c, PDL1, CD80, CD86, and IFN-γ were purchased from eBioscience (San Diego, CA).

Cell Line and Medium

TAg-transformed B6/WT-19 cells have been described previously.[24] The cell line was maintained in Dulbecco's modified Eagle medium (DMEM; Cellgro, Manassas, VA) supplemented with 100 U/mL penicillin, 100 μg/mL streptomycin, 100 μg/mL kanamycin, 2 mmol/L L-glutamine, 10 mmol/L HEPES, 0.075% (w/v) $NaHCO_3$, and 10% fetal bovine serum (FBS) at 37°C in a 5% CO_2 humidified atmosphere.

Preparation of Clinically Relevant Murine Model of HCC

To model tumor growth in a fibrotic liver, 10% CCl_4 (v/v) solution in corn oil was intraperitoneally (IP) injected into 6-week-old C57BL/6 mice twice a week at a dose of 8 mL/kg of body weight for 6 weeks.[17] Two weeks after the last injection, the mice received intrasplenic innoculation of histologically normal hepatocytes isolated from TAg-transformed young male MTD2 mice at a dose of 5×10^5 cells/mouse. At the onset of puberty, the generation of androgens in the recipient mice initiated oncogenic TAg expression under control of a liver-specific promoter. As a result, the transferred hepatocytes became cancer cells and formed tumors in the setting of liver fibrosis/cirrhosis. Small tumors can be detected by magnetic resonance imaging (MRI) 2 months after hepatocyte inoculation.

LipC6 Injection, Adoptive Cell Transfer, and Immunization

LipC6 or vehicle were injected via tail vein every other day for 2 weeks at dose of 35 mg/kg body weight in 200 μl volume. For adoptive cell transfer (ACT), TCR-I cells were isolated from the spleens of line 416 mice and enriched by $CD8^+$ magnetic microbeads (Miltenyi Biotech, Auburn, CA) according to the manufacturer's instructions. 1×10^6 TCR-I^+ T cells were suspended in 0.2 mL of HBSS and injected into the mice via tail vein. For

immunization, 3×10^7 B6/WT-19 cells suspended in 0.2 mL of phosphate-buffered saline were IP injected to mice.

Isolation of Leukocytes From Liver or Tumors

To isolate liver- or tumor-infiltrating leukocytes (TIL), a liver perfusion was first performed via the portal vein with 15 mL collagenase IV (Sigma, St. Louis, MO) solution. The harvested tumor or live tissues were cut to small pieces and incubated in mixed enzymes including collagenase IV, hyaluronidase, and DNase IV (Sigma) at room temperature; 1.5 hours later, lower speed centrifugation, RBC lysis, and the gradient centrifugation were used to isolate leukocytes. These cells were maintained in RPMI 1640 medium (Cellgro) supplemented with 100 U/mL penicillin, 2 mmol/L L-glutamine, 10 mmol/L HEPES, 50 μmol/L 2-mercaptoethanol, and 10% FBS.

Flow Cytometry

Ex vivo staining of leucocytes with fluorochrome-labeled antibodies was performed on single-cell suspensions.[25] Stained cells were analyzed using Accuri C6 flow cytometer (BD Biosciences, San Jose, CA). Data were analyzed using FlowJo software (Tree Star; https://www.flowjo.com/). Staining of intracellular IFN-γ and TNF-α was performed as described previously.[25] Staining of FoxP3 was performed with a buffer set from eBioscience.

Preparation of Bone Marrow-derived Macrophages

Bone marrow was harvested from the femurs and tibias of C57BL/6 mice. RBCs were lysed with lyse buffer (eBioscience). 3×10^6 single cells were then plated in a 100-mm petri dish and cultured in 10 mL DMEM medium (Cellgro) supplemented with 10% FBS, 10 mmol/L HEPES, 1:100 (v/v) non-essential amino acids, 1 mmol/L sodium pyruvate (Sigma), and 20 ng/mL mouse macrophage colony-stimulating factor (MCSF) or mouse granulocyte macrophage colony-stimulating factor (GMCSF) (R&D System, Minneapolis, MN). Five mL fresh complete medium containing 20 ng/mL mouse macrophage colony-stimulating factor or granulocyte macrophage colony-stimulating factor was added to the culture cells on day 4. Adherent cells were harvested on day 7 and used as BMMs.

ELISA

The level of IFN-γ in cell culture supernatant was measured with mouse Quantikine ELISA Kits (Cat # DY485, R&D System) according to the manufacturer's instructions.

ROS Detection Assay

ROS level was detected and quantified using the ROS-Glo H_2O_2 Assay (Promega, Madison, WI) according to the manufacturer's protocol. Briefly, cells were grown in 96-well plate until 80% confluence followed by the incubation with LipC6 or vehicle for 6 hours, the H_2O_2 substrate was added to each well and incubated in 37°C, 5% CO_2 incubator for desired time, then ROS-Glo detection solution was added and incubated for 20 minutes at room temperature. Luminescence intensity was quantified using a microplate reader and normalized to control cells.

Total RNA Extraction and Real-time PCR

Total RNAs were extracted using Trizol reagent (Invitrogen, Carlsbad, CA) according to the manufacturer's instructions. Two μg of total RNAs were used for cDNA synthesis with High Capacity cDNA Reverse Transcription Kits (Applied Biosystems, Foster City, CA). Each PCR was performed in a 20-μL reaction mixture containing SYBR Green I (Roche, Basel, Switzerland). Real-time PCR was performed with CFX96 Real-Time PCR Detection System (Bio-Rad, Hercules, CA). Reactions were run in triplicate in 3 independent experiments. Expression data were normalized to the geometric mean of housekeeping gene 18S rRNA to control the variability in expression levels and were analyzed using the $2^{-\Delta\Delta CT}$ method.

Primers for Real-time PCR

Primers were synthesized by Fisher Scientific (Waltham, MA). The sequences are shown in Supplementary Table 1.

Statistics Analysis

Paired data were analyzed using a 2-tailed paired Student's *t* test. A *P* value of <.05 was considered significant.

Study Approval

Animal experiments were approved by the Institutional Animal Care and Use Committee of the Pennsylvania State University College of Medicine (Hershey, PA), the Medical University of South Carolina (Charleston, SC), and the University of Missouri (Columbia, MO).

Results

LipC6 Promotes Elimination of Established Tumors in Combination With tumor antigen-specific CD8$^+$ T Cells and Immunization

We evaluated the therapeutic efficacy of LipC6 monotherapy and its combination with immunotherapy in our clinically relevant HCC model. Naïve TCR-I T cells isolated from line 416 mice served as tumor antigen-specific (TAS) CD8$^+$ T cells that specifically recognize TAg-epitope-I. B6/WT-19 cells served as tumor-specific antigens that express full-length wild-type TAg. Size-matched tumor-bearing mice (TBMs) were randomly assigned to 6 groups and received the following administrations: LipC6 injection; LipC6 injection followed by immunization; LipC6 followed by ACT and immunization (Figure 1*A*). Parallel 3 control groups of mice were injected with vehicle instead of LipC6. Fluorescence detection indicated that Rhodamine-labeled LipC6 mainly distributed in the spleen and liver (Supplementary Figure 2*A*). Electron micrographs of tumor sections confirmed that LipC6 particles mainly localize to tumor cells, macrophages, and liver sinusoidal endothelial cells (Supplementary Figure 2*B*). These suggest that LipC6 may be specifically appropriate for the therapy of HCC. MRI was used to monitor therapeutic efficacy by assessing initial tumor volume and subsequent tumor growth (Figure 1*B*, 1*C*). In 3 vehicle-related cohorts, tumors continued to progress after initial injection with > 700% increase in tumor size by week 6 (Figure 1*B*–*D*). In contrast, LipC6 monotherapy slowed tumor growth, resulting in < 300%

increase in tumor size within the 6-week administration period. The combination of LipC6 and immunization was more effective with < 180% increase in tumor size over 6 weeks of administration (Figure 1*B–D*). Importantly, LipC6-integrated triple combination therapy not only retarded tumor growth, but eventually led to regression of established tumors (Figure 1*B–D*). Collectively, these data demonstrate that LipC6 synergizes with immunotherapy to powerfully suppress tumor growth that is involved in LipC6's mediated immune activation. LipC6's therapeutic and immunomodulatory effect were also detected in an N-nitrosodiethylamine (DEN)-induced HCC model (Supplementary Figure 3).

LipC6 Injection Preserves the TAS Effector T-Cell Response

Considering the enhanced tumoricidal effect of LipC6-integrated immunotherapy relative to control mono-therapies with LipC6 or immunotherapy alone, we hypothesized that LipC6 may be able to prime therapeutic antitumor immune response. To test this hypothesis, HCC-bearing mice were assigned into 3 groups: vehicle, LipC6, and no injection. Following the injection, each mouse in the 3 groups received ACT of naïve TAS TCR-I T cells labeled with carboxyfluorescein succinimidyl ester (CFSE). Half of the mice in each group received TAS immunization with B6/WT-19 cells. Seven days after immunization, CFSE dilution was observed in TCR-I T cells recovered from the spleens of all 3 groups of TBMs, suggesting that proliferation of naïve TCR-I T cells occurred after initial interaction with tumor antigens without the need for immunization. However, further expansion of TCR-I T cells in response to TAS immunization were only detected in the LipC6-injected TBMs, with 0.28% $CFSE^+CD8^+$ T cells observed in immunized mice vs 0.18% in unimmunized mice (Figure 2*A* and Supplementary Figure 4*A*). In addition, the expansion of TCR-I T cells was accompanied by their differentiation to effector cells. In vitro short-term exposure to epitope-I peptide revealed an increase in the frequency of $CD8^+$ T cells producing IFN-γ (0.36% IFN-γ^+CD8^+T cells) in LipC6-injected and immunized mice, which was equivalent to that observed in immunized normal mice and much higher than that in control HCC-bearing mice without injection (0.085% IFN-γ^+CD8^+T cells) or vehicle-injected mice (0.15% IFN-γ^+CD8^+T cells) (Figure 2*B* and Supplementary Figure 4*B*). These results indicate that LipC6 injection protects TAS $CD8^+$ T cells in TBMs, maintaining their potential for response to immunization.

Next, we investigated whether LipC6 injection influences the phenotype of $CD8^+$ TILs. Flow cytometry analysis showed that tumor growth induced noticeable increase in the frequency of $CD8^+$TILs expressing PD-1 (15.7%) compared with that in tumor-free mice (0.72%). In vivo injection of TBMs with LipC6 resulted in remarkable reduction in the frequency of PD-1^+CD8^+TILs (4.97%) (Figure 2 and Supplementary Figure 4*C*). However, LipC6 injection did not similarly reduce the frequency $CD4^+$TILs expressing PD-1 (Figure 2*D* and Supplementary Figure 4*D*). Collectively, these data suggest that LipC6 injection modulates effector $CD8^+$ T cells phenotypically and functionally.

Because LipC6 injection increased the accumulation of functional TAS $CD8^+$ T cells and also reduced the population of PD-1^+TILs, we investigated if PD-1 blockade could improve TIL activity. TILs isolated from TBMs were stimulated with anti-CD3 and anti-CD28 for 48 hours in the presence or absence of anti-PD-1 antibodies. The supernatant was harvested to

measure IFN-γ production by ELISA. The results showed that anti-PD-1 significantly enhanced IFN-γ production in TILs from 500 pg/mL to 1200 pg/mL (Figure 2*E*). These data suggest that LipC6 may improve the function of TILs through suppression of PD-1 expression.

LipC6's Inherent Tumoricidal Properties

Our previous in vitro studies indicated that AKT phosphorylation mediates the resistance of HCC cells to apoptosis.[16] We found that HCCs also express high levels of phosphorylated AKT that could be down-regulated by LipC6 injection (Supplementary Figure 5). In addition, LipC6 injection was found to decrease levels of Ki67 and CD31 but increase levels of cleaved caspase 3 and necrosis (Figure 2*F*). These results indicate that LipC6 monotherapy suppresses tumor cell proliferation and vascularization but increases apoptosis and necrosis. Together, the in vitro and in vivo findings suggest LipC6's inherent tumoricidal effect on HCCs is, at least in part, because of its suppression of Akt signaling.

LipC6 Injection Modulates the Frequency and Function of TAMs in TBMs

We next investigated the impact of LipC6 injection on immunosuppressive cell subsets in TBMs, including typically recognized $CD11b^+Gr\text{-}1^+$ myeloid-derived suppressor cells (MDSCs), $CD4^+CD25^+FoxP3^+$regulatory T cells (Tregs), and $CD11b^+F4/80^+$ TAMs.[26,27] Flow cytometry analysis indicated that tumor progression led to a significant increase in the frequency of MDSCs (Figure 3*A*), Tregs (Figure 3*B*), and TAMs (Figure 3*C*) in TILs compared with normal mice. LipC6 injection significantly reduced the magnitude of TAMs from 15% to 4% (Figure 3*B*, Supplementary Figure 6), but has little impact on the frequency of MDSCs (Figure 3*A*) and Tregs (Figure 3*B*). ELISA analysis suggested that anti-CD3 and anti-CD28 were unable to effectively stimulate IFN-γ secretion in the mixed TILs from mice without LipC6 injection (700 pg/mL) or vehicle injection (400 pg/mL) (Figure 3*D*). In contrast, LipC6 injection resulted in a significant increase in IFN-γ production (1700 pg/mL) in TILs. Next, TAMs were isolated from TILs (> 90% isolated cells expressed $CD11b^+$). Isolated TAMs were co-cultured with responder cells from macrophage-depleted splenocytes of wild-type mice. In response to stimulation with anti-CD3 and anti-CD28, TAMs from mice with vehicle or no injection largely suppressed IFN-γ production in responder cells (Figure 3*E*). In contrast, LipC6 injection blocked TAMs' suppressive effect and enabled responder cells to produce 1800 pg/mL IFN-γ, equivalent to 1700 pg/mL produced in the presence of macrophages from normal mice (Figure 3*E*). These results suggest that LipC6 injection reduces not only TAM frequency but also its suppressive function.

LipC6 Injection Results in Reduced Expression of M2-like Markers in TAMs

To document whether LipC6-induced alteration in TAMs may be accompanied by a shift in TAM phenotype, TILs were isolated from TBMs that received vehicle, LipC6, or no injection, then labeled with markers associated with classically activated (M1) or alternatively activated (M2) macrophages to conduct flow cytometry. Compared with normal mice, tumor growth induced an increase in the frequency of $CD11b^+F4/80^+$ macrophages (Figure 4*A*) that contains a higher proportion of cells expressing M2 macrophage markers, including CD11c (Figure 4*B*) and PD-L1 (Figure 4*C*), while there was slight alteration in the

expression of the M1 marker CD80 (Figure 4*D*) and CD86 (Figure 4*E*). LipC6 injection remarkably reduced the expression of CD11c (Figure 4*B*) and PD-L1 (Figure 4*C*) in CD11b $^{+}$F4/80^{+}macrophages to the level seen in normal mice, but minimally altered the expression of CD80 (Figure 4*D*) and CD86 (Figure 4*E*). These data suggest that LipC6 injection suppresses the expression of M2-like markers in TAMs. Real-time PCRs suggest that LipC6 injection led to an increased mRNA expression of CD80 and CD86, reduced mRNA expression of CD11c, but no change was detected in PD-1 mRNA expression in TAMs (Figure 4*F*). These results are not entirely consistent with the levels of protein expression, suggesting the likely translational regulation of PD-L1, CD80, and CD86.

LipC6 Injection Results in Reduced ROS Production by TAMs

To elucidate the mechanism by which LipC6 phenotypically and functionally modulates TAMs, we investigated the injection of LipC6 on ROS production, a critical factor in modulation of TAMs.[22] Using a luminescent assay, we found a 60% decrease in ROS production in TAMs from LipC6-injected TBMs (Figure 5*A*) and a 30% reduction in vehicle-injected mice relative to control mice without injection. A similar reduction in ROS was observed in macrophages isolated from the spleen of TBMs with LipC6 injection (Figure 5*B*).

To investigate whether LipC6 similarly modulates ROS production in M1 macrophages and M2 macrophages, we generated M1-like or M2-like BMMs by stimulating bone marrow cells from wild-type C57BL/6 mice with GMCSF or MCSF.[28,29] Subsequently, BMMs were incubated with LipC6 for 24 hours at a selected dose of 25 μmol/L (Supplementary Figure 7), then ROS levels in M1 or M2 BMMs was measured. We found that LipC6 incubation significantly blocked ROS production in both GMCSF-induced M1 BMMs (Figure 5*C*) and MCSF-induced M2 BMMs (Figure 5*D*). This suppressive effect on ROS production was only detected in C6- and C8-ceramides in contrast to the longer chain ceramide species (Supplementary Figure 8). We speculate that exogenous chain species have optimal biophysical properties to intercalate into macrophages and induce structured membrane micro domains. Thus, both in vivo and in vitro data suggest that LipC6 significantly suppresses ROS production independent of macrophage phenotypes. The further studies indicate that interferon-regulatory factors (IRFs) may represent an underlying molecular mechanism. We found that LipC6 injection significantly regulate IRF1, 2, 3, and 6 in TAMs; furthermore, these results were validated by ex vivo incubation of TAMs with LipC6 (Supplementary Figure 9).

LipC6 Enhances M1 Cytokine Production and Inhibits M2 Cytokine Production in Mouse BMMs

To investigate whether LipC6 incubation differentially regulates enzyme and cytokine production in GMCSF-induced M1 and MCSF-induced M2 BMMs, M1 and M2 BMMs were incubated with LipC6 or vehicle for 24 hours. Real-time PCRs indicated that LipC6 incubation significantly promoted production of enzyme iNOS (Figure 6*A*) and M1 cytokines in M1 BMMs, including IL12 (Figure 6*B*), IFN-γ (Figure 6*C*), and TNF-α (Figure 6*D*). Conversely, LipC6 incubation significantly suppressed the production of enzyme Arg1 (Figure 6*E*) and M2 cytokine in M2 BMMs, including IL4 (Figure 6*F*), Fizz

(Figure 6*G*), and Ym1 (Figure 6*H*). These data suggest that LipC6 promoted M1 activation in GMCSF-induced BMMs but suppressed M2 activation in MCSF-induced M2 BMMs.

ROS are Required for LipC6-mediated Modulation of Macrophages

To further investigate whether ROS are a critical regulator in LipC6-mediated modulation of macrophages, bone marrow-derived monocytes were stimulated with MCSF for 6 hours followed by incubation with LipC6 for 2 hours in the presence or absence of H_2O_2. Flow cytometric analysis demonstrated that the addition of H_2O_2 compensated LipC6-mediated reduction in the expression of PD-L1 and CD11c (Figure 7*A*) in the resultant cells. To further study if ROS signaling is required for LipC6-mediated modulation of macrophages, we compared the function of LipC6 and the ROS specific inhibitor N-acetyl-L-cysteine (NAC) in modulating M1 cytokine production in GMCSF-induced macrophages. Detection of different cytokine mRNAs with real-time PCR showed that LipC6 incubation resulted in increased M1 cytokine production including iNOS, IL12, IFN-γ, and TNF-α (Figure 7*B*–*E*). This profile was similar to that induced by NAC incubation. In addition, the combination of LipC6 and NAC had a greater effect than either compound alone. Taken together, these results suggest LipC6 modulates BMMs by inhibiting ROS signaling.

Discussion

The present studies reveal a novel role of LipC6 in breaking tumor-induced immunotolerance in HCC, which is confirmed by eradication of established tumors via its combination with an ACT and immunization approach. The inherent p-AKT–dependent tumoricidal activity of ceramide together, with the ability to reverse tumor-induced immunotolerance, offers the promise of utilizing LipC6 as a significant anticancer therapeutic component that can be integrated into cancer immunotherapy.

Our data show that LipC6 has immunomodulatory effects in addition to its inherent tumoricidal properties. This result is consistent with a previous report indicating that the antitumor activity of some conventional drugs is, in part, associated with their ability to re-activate the anti-tumor immune response.[30] Our current findings suggest that development of LipC6-combined strategy, which both maximizes tumor control and facilitates antitumor immune activity, are expected to achieve long-term clinical benefit in HCC.[31–33] As shown in our current studies, LipC6 mono-therapy decreases tumor growth but was unable to eliminate tumors or block further progression. Integration of LipC6 with TAS ACT and immunization resulted in the regression of established tumors (Figure 1*A*–*D*). These results suggest that LipC6 injection effectively blocks anergy of effector $CD8^+$ T cells, allowing the response to immunization to exert cytotoxic function against established tumors. This immunomodulatory function on TAS $CD8^+$ T cells may be generated by LipC6's indirect effect because no direct activation was detected in LipC6-administrated TAS TCR-I T cells (Supplementary Figure 10). Therefore, LipC6 is not only a tumoricidal reagent, but also a strong immunomodulatory factor. These synergistic anti-tumor activities plus the clinically feasible delivery of nanolipsomes highlight the considerable potential for LipC6-intergrated immunotherapies to translate into therapy for HCC and other cancers.

Ceramide plays important roles in both cell structure and signaling in multiple cell types, including immune cells.[34] Our group has shown that LipC6 exerts tumoricidal activity in HCC[16] and other cancers.[19,35,36] Extensive pre-clinical evaluation of LipC6 has been led to the very recent approval of the investigational new drug application regarding its safety in patients with solid tumors (109471). Also, no toxicity was detected in LipC6-administrated HCC-bearing mice by evaluating liver enzymes, kidney function, hematologic toxicity (Supplementary Figure 11) and cardiac toxicity (data not shown). However, very little is known about the function of ceramide in antitumor immunity. We found that LipC6 injection blocks the onset of tolerance of TAS $CD8^+$ T cell in the setting of HCC, and facilitates increased proliferation and IFN-γ production in response to tumor antigen stimulation (Figure 2). Consistent with our finding, a recent publication reports that conditioning of lymphocytic choriomeningitis virus-infected mice with C8 ceramide enhances the T-cell response to virus infection by promoting the expansion of virus-specific $CD8^+$ T cells.[37] A previous study suggested that the ceramide-metabolizing enzyme acid sphingomyelinase plays an important role in T-cell degranulation by increasing ceramide.[38] In contrast to this immune stimulatory activity, 1 group reported that exogenous addition of ceramide was reported to inhibit antigen uptake by dendritic cells and impair their capability to stimulate Ag-specific T cells.[39] However, the dendritic cells used in the study were prepared from healthy donors. These contradictory effects suggest that ceramides may differently impact immune response in healthy subjects and cancer patients.

Our data indicate that LipC6 activates antitumor immunity by targeting TAM through regulating ROS signaling. Our in vivo studies suggest that injection of TBMs with LipC6 results in the reduction of both the frequency of TAMs (Figure 3*B–D*) and the expression of M2-like markers (Figure 4) as well as the immunosuppressive function (Figure 3). In vitro studies with BMMs validate that LipC6 can phenotypically (Figure 7) and functionally (Figure 6) modulate BMMs. Furthermore, addition of H_2O_2 blocks the LipC6-induced shift in macrophage phenotype from M2 to M1 (Figure 7*A*); incubation of BMMs with LipC6 and NAC, a ROS-specific inhibitor, generates similar response profiles (Figure 7*B*). These data suggest that macrophages are an important target of LipC6 and that ROS is a critical signal that is neutralized to overcome the effect of tumor-induced immunotolerance. Consistent with our findings, a recent report demonstrates that the continuous injection of the ROS inhibitor butylated hydroxyanisole (BHA) efficiently blocks the accumulation of TAMs and markedly suppresses tumorigenesis in lung cancer mouse models.[22] In particular, ROS production was shown to be important in M2 but not M1 macrophage differentiation. It also has been reported that ROS is a critical trigger of Cox-2–mediated macrophage differentiation from monocytes. Studies on oxidative stress-linked endotoxic shock suggest that NAC injection provides a therapeutic effect by modulating the function of macrophages and decreasing the production of ROS. Collectively, these results indicate that LipC6 functions as a ROS scavenger to alter macrophage functionality in the TME. In the present study, we noted a small but significant ROS change in TAMs from vehicle-injected TBMs. Vehicle contains an equal amount of lipid components in the same ratio as LipC6, except without ceramide. This finding is consistent with previous reports regarding the effect of liposomes on mouse liver macrophages.[40] However, it should be noted that in all

circumstances this effect is less than LipC6 and not statistically significant. In fact, vehicle formulations did not change any of the other parameters measured in the current study.

Our present studies also showed that LipC6 reduced PD-L1 expression in TAMs, and neutralization of PD-1 in TILs with anti-PD-1 antibodies increased IFN-γ production in TILs, suggesting PD-1 signaling may represent another mechanism through which LipC6 overcomes tumor-induced immune suppression. We recently demonstrated that a chemoimmunotherapy modality with combination of anti-PD-1 and US Food and Drug Administration-approved sunitinib, a tyrosine kinase inhibitor, strongly suppressed HCC growth.[17] Therefore, integration of LipC6 with anti-PD-1 or other kinds of immunotherapies is deserving of further evaluation for development of a clinically available therapeutic modality in the treatment of HCC. In summary, the current work provides new insight into the mechanisms by which LipC6 abrogates tumor-induced immune tolerance and demonstrates the potential for LipC6-integrated immunotherapeutic approaches to expand treatment options for patients with HCC.

Supplementary Material

Refer to Web version on PubMed Central for supplementary material.

Acknowledgments

The authors thank Patti Miller, Pennsylvania State University College of Medicine, and Xingju Nie, Medical University of South Carolina, for their assistance in monitoring tumors with MRI.

Grant support

1 R01 CA164335-01A1 (K.F. Staveley-O'Carroll, PI) and R01CA208396 (M. Kester, G. Li, and K.F. Staveley-O'Carroll).

Abbreviations used in this paper

ACT	adoptive cell transfer
BMM	bone marrow-derived macrophage
CFSE	carboxyfluorescein succinimidyl ester
DEN	N-nitrosodiethylamine
GMSCF	granulocyte-macrophage colony-stimulating factor
HCC	hepatocellular cancer
IP	intraperitoneal
LipC6	nanoliposome-loaded C6-ceramide
MCSF	macrophage colony-stimulating factor
MDSC	myeloid-derived suppressor cell
MRI	magnetic resonance imaging

NAC	N-acetyl-L-cysteine
ROS	reactive oxygen species
TAg	SV40 T antigen
TAM	tumor-associated macrophage
TAS	tumor antigen-specific
TBM	tumor-bearing mice
TCR	T-cell receptor
TCR-I T cells	TAg-specific $CD8^+$ T cells
TIL	tumor-infiltrating leukocyte
TME	tumor microenvironment
Treg	regulatory T cell

References

Author names in bold designate shared co-first authorship.

1. Forner A, Llovet JM, Bruix J. Hepatocellular carcinoma. Lancet. 2012; 379:1245–1255. [PubMed: 22353262]
2. Gajewski TF, Schreiber H, Fu YX. Innate and adaptive immune cells in the tumor microenvironment. Nat Immunol. 2013; 14:1014–1022. [PubMed: 24048123]
3. Mueller KL. Cancer immunology and immunotherapy. Realizing the promise. Introduction Science. 2015; 348:54–55. [PubMed: 25838372]
4. Niu LZ, Li JL, Zeng JY, et al. Combination treatment with comprehensive cryoablation and immunotherapy in metastatic hepatocellular cancer. World J Gastroenterol. 2013; 19:3473–3480. [PubMed: 23801841]
5. Gajewski TF, Schumacher T. Cancer immunotherapy. Curr Opin Immunol. 2013; 25:259–260. [PubMed: 23587868]
6. Ribas A, Wolchok JD. Combining cancer immunotherapy and targeted therapy. Curr Opin Immunol. 2013; 25:291–296. [PubMed: 23561594]
7. Pembrolizumab superior to ipilimumab in melanoma. Cancer Discov. 2015; 5:568.
8. Breous E, Thimme R. Potential of immunotherapy for hepatocellular carcinoma. J Hepatol. 2011; 54:830–834. [PubMed: 21145836]
9. Liu D, Staveley-O'Carroll KF, Li G. Immune-based therapy clinical trials in hepatocellular carcinoma. J Clin Cell Immunol. 2015:6.
10. Schneider C, Teufel A, Yevsa T, et al. Adaptive immunity suppresses formation and progression of diethylnitrosamine-induced liver cancer. Gut. 2012; 61:1733–1743. [PubMed: 22267597]
11. Greten TF, Wang XW, Korangy F. Current concepts of immune based treatments for patients with HCC: from basic science to novel treatment approaches. Gut. 2015; 64:842–848. [PubMed: 25666193]
12. Morad SA, Cabot MC. Ceramide-orchestrated signalling in cancer cells. Nat Rev Cancer. 2013; 13:51–65. [PubMed: 23235911]
13. Morales A, Lee H, Goni FM, et al. Sphingolipids and cell death. Apoptosis. 2007; 12:923–939. [PubMed: 17294080]

14. Pettus BJ, Chalfant CE, Hannun YA. Ceramide in apoptosis: an overview and current perspectives. Biochim Biophys Acta. 2002; 1585:114–125. [PubMed: 12531544]
15. Stoffel B, Bauer P, Nix M, et al. Ceramide-independent CD28 and TCR signaling but reduced IL-2 secretion in T cells of acid sphingomyelinase-deficient mice. Eur J Immunol. 1998; 28:874–880. [PubMed: 9541582]
16. Tagaram HR, Divittore NA, Barth BM, et al. Nanoliposomal ceramide prevents in vivo growth of hepatocellular carcinoma. Gut. 2011; 60:695–701. [PubMed: 21193455]
17. Li G, Liu D, Cooper TK, et al. Successful chemoimmunotherapy against hepatocellular cancer in a novel murine model. J Hepatol. 2017; 66:75–85. [PubMed: 27520877]
18. Kester M, Bassler J, Fox TE, et al. Preclinical development of a C6-ceramide NanoLiposome, a novel sphingolipid therapeutic. Biol Chem. 2015; 396:737–747. [PubMed: 25838296]
19. Liu X, Ryland L, Yang J, et al. Targeting of survivin by nanoliposomal ceramide induces complete remission in a rat model of NK-LGL leukemia. Blood. 2010; 116:4192–4201. [PubMed: 20671121]
20. Zolnik BS, Stern ST, Kaiser JM, et al. Rapid distribution of liposomal short-chain ceramide in vitro and in vivo. Drug Metab Dispos. 2008; 36:1709–1715. [PubMed: 18490436]
21. Sica A, Invernizzi P, Mantovani A. Macrophage plasticity and polarization in liver homeostasis and pathology. Hepatology. 2014; 59:2034–2042. [PubMed: 24115204]
22. Zhang Y, Choksi S, Chen K, et al. ROS play a critical role in the differentiation of alternatively activated macrophages and the occurrence of tumor-associated macrophages. Cell Res. 2013; 23:898–914. [PubMed: 23752925]
23. Held WA, Mullins JJ, Kuhn NJ, et al. T antigen expression and tumorigenesis in transgenic mice containing a mouse major urinary protein/SV40 T antigen hybrid gene. EMBO J. 1989; 8:183–191. [PubMed: 2714250]
24. Staveley-O'Carroll K, Schell TD, Jimenez M, et al. In vivo ligation of CD40 enhances priming against the endogenous tumor antigen and promotes CD8+ T cell effector function in SV40 T antigen transgenic mice. J Immunol. 2003; 171:697–707. [PubMed: 12847236]
25. Avella DM, Li G, Schell TD, et al. Regression of established hepatocellular carcinoma is induced by chemoimmunotherapy in an orthotopic murine model. Hepatology. 2012; 55:141–152. [PubMed: 21898502]
26. Duluc D, Delneste Y, Tan F, et al. Tumor-associated leukemia inhibitory factor and IL-6 skew monocyte differentiation into tumor-associated macrophage-like cells. Blood. 2007; 110:4319–4330. [PubMed: 17848619]
27. Zou W. Immunosuppressive networks in the tumour environment and their therapeutic relevance. Nat Rev Cancer. 2005; 5:263–274. [PubMed: 15776005]
28. Fleetwood AJ, Dinh H, Cook AD, et al. GM-CSF- and M-CSF-dependent macrophage phenotypes display differential dependence on type I interferon signaling. J Leukoc Biol. 2009; 86:411–421. [PubMed: 19406830]
29. Martinez FO, Gordon S, Locati M, et al. Transcriptional profiling of the human monocyte-to-macrophage differentiation and polarization: new molecules and patterns of gene expression. J Immunol. 2006; 177:7303–7311. [PubMed: 17082649]
30. Emens LA. Chemoimmunotherapy. Cancer J. 2010; 16:295–303. [PubMed: 20693839]
31. Mapara MY, Sykes M. Tolerance and cancer: mechanisms of tumor evasion and strategies for breaking tolerance. J Clin Oncol. 2004; 22:1136–1151. [PubMed: 15020616]
32. Melief CJ, Toes RE, Medema JP, et al. Strategies for immunotherapy of cancer. Adv Immunol. 2000; 75:235–282. [PubMed: 10879286]
33. Sharma P, Wagner K, Wolchok JD, et al. Novel cancer immunotherapy agents with survival benefit: recent successes and next steps. Nat Rev Cancer. 2011; 11:805–812. [PubMed: 22020206]
34. Spiegel S, Milstien S. The outs and the ins of sphingosine-1-phosphate in immunity. Nat Rev Immunol. 2011; 11:403–415. [PubMed: 21546914]
35. Watters RJ, Fox TE, Tan SF, et al. Targeting gluco-sylceramide synthase synergizes with C6-ceramide nanoliposomes to induce apoptosis in natural killer cell leukemia. Leuk Lymphoma. 2013; 54:1288–1296. [PubMed: 23181473]

36. Jiang Y, DiVittore NA, Kaiser JM, et al. Combinatorial therapies improve the therapeutic efficacy of nano-liposomal ceramide for pancreatic cancer. Cancer Biol Ther. 2011; 12:574–585. [PubMed: 21795855]

37. Pritzl CJ, Seo YJ, Xia C, et al. A ceramide analogue stimulates dendritic cells to promote T cell responses upon virus infections. J Immunol. 2015; 194:4339–4349. [PubMed: 25810392]

38. Herz J, Pardo J, Kashkar H, et al. Acid sphingomyelinase is a key regulator of cytotoxic granule secretion by primary T lymphocytes. Nat Immunol. 2009; 10:761–768. [PubMed: 19525969]

39. Sallusto F, Nicolo C, De Maria R, et al. Ceramide inhibits antigen uptake and presentation by dendritic cells. J Exp Med. 1996; 184:2411–2416. [PubMed: 8976196]

40. Moghimi SM, Patel HM. Modulation of murine liver macrophage clearance of liposomes by diethylstilbestrol. The effect of vesicle surface charge and a role for the complement receptor Mac-1 (CD11b/CD18) of newly recruited macrophages in liposome recognition. J Control Release. 2002; 78:55–65. [PubMed: 11772449]

EDITOR'S NOTES

BACKGROUND AND CONTEXT

Nano-formulation of C6-ceramide (LipC6) has been demonstrated to reduce tumor vascularization and tumor growth, but LipC6's effect in preventing tumor-induced immune tolerance in hepatocellular cancer (HCC) remains to be studied.

NEW FINDINGS

The researchers demonstrate LipC6 treatment activates therapeutic antitumor immune by phenotypically and functionally modulates tumor-associated macrophages (TAMs).

LIMITATIONS

This study did not test the effect of LipC6 in modulating antitumor immune response in patients with HCC.

IMPACT

New finding into ability of LipC6 in modulating antitumor immunity provides a rationale of developing LipC6-integrated immunotherapy in the treatment of HCC.

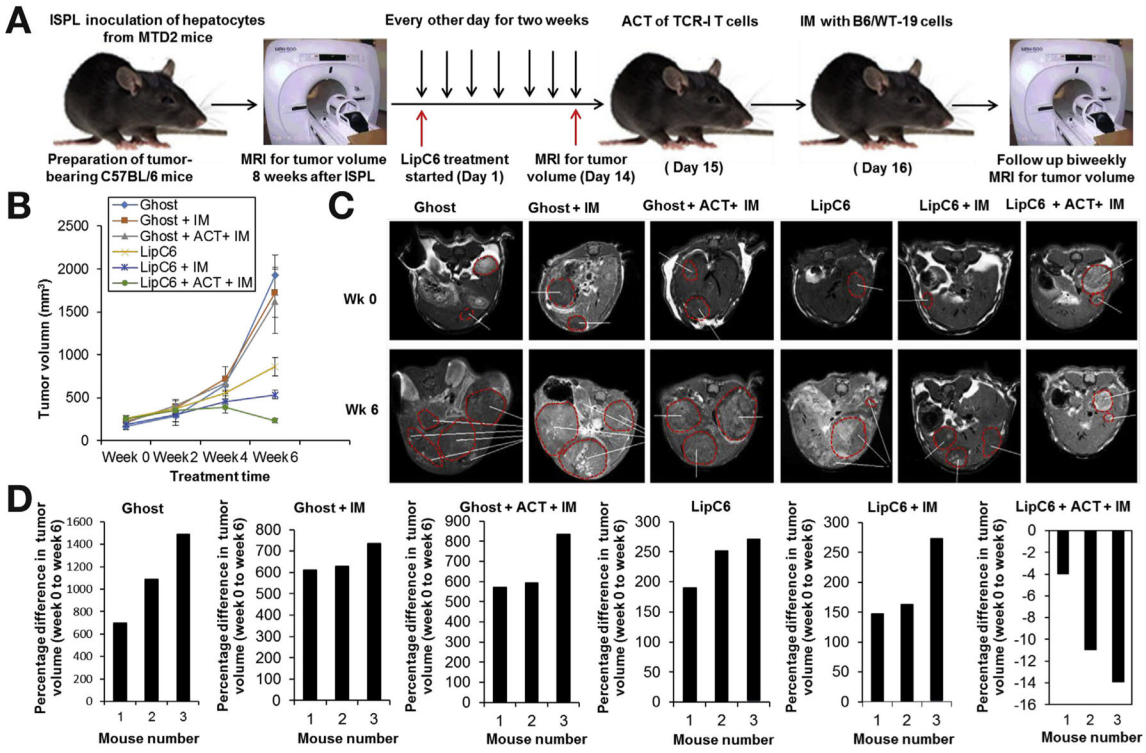

Figure 1.

LipC6 injection in combination with TAS ACT and immunization blocks tumor growth and effectively abolishes established HCC tumors. (*A*) Experimental design for therapeutic trial in TBMs. Mice bearing tumors detectable by MRI were randomly assigned to 1 of 6 groups and received the indicated administrations. (*B*) Mean tumor volume in mice over the experiment time is shown. Starting tumor volumes for each mouse was about 120 mm^3. (*C*) Representative images of MRI scans to detect tumors from the start to endpoints are shown. The tumors in images are shown by red dashed lines. (*D*) Waterfall plots showing the change in tumor volume at the experimental endpoint relative to the starting tumor volume for each mouse. In 3 vehicle-injected control groups, there was a progressive, substantial increase in tumor growth ranging from 600% to about 1500%. In 3 LipC6 injection-integrated groups, tumor growth was reduced, especially the combination of LipC6 with TCR-I, and immunization resulted in about 10% reduction in tumor volume. n = 6; error bars represent means ± SD.

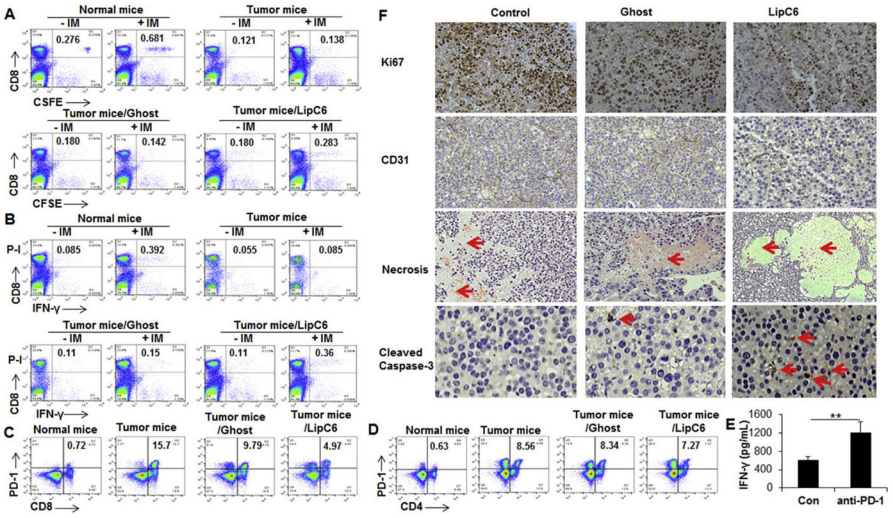

Figure 2.

LipC6 injection restores exhausted $CD8^+$ T-cell function in HCC and exerts tumoricidal effect. Size-matched TBMs were randomly assigned into 1 of 3 groups: vehicle, LipC6, or no injection. Two weeks after injection, mice received ACT of 1×10^6 naïve TAS TCR-I T cells that were labeled by CFSE. On the second day, half of the mice in each group were immunized, as in Methods section, with TAg-transformed B6/WT-19 cells. Seven days after TAS immunization, spleens were harvested and splenic lymphocytes were isolated. Wild-type C57BL/6 mice with or without immunization were used as controls. CFSE dilution in TCR-I T cells was detected by flow cytometry after labeling cells with anti-CD8 (*A*). IFN-γ production in effector $CD8^+$ T cells upon short-term exposure to peptide I was detected by flow cytometry after labeling with anti-CD8 and IFN-γ (*B*). Expression of PD-1 in $CD8^+$ TILs (*C*) and $CD4^+$ T TILs (*D*) was detected after labeling cells anti-CD4, CD8 and PD-1. In vitro incubation with anti-PD1 antibody increases the IFN-γ production in TILs (*E*). Immunohistochemistry and H&E staining were used to detect the level of Ki67, CD31, cleaved caspase-3, and necrosis in tumors from each mouse with the indicated monotherapies (*F*). The results implied that in vivo injection with LipC6 suppressed tumor cell proliferation and vascularization, but increased apoptosis and necrosis. Data are representative of 3 independent analyses.

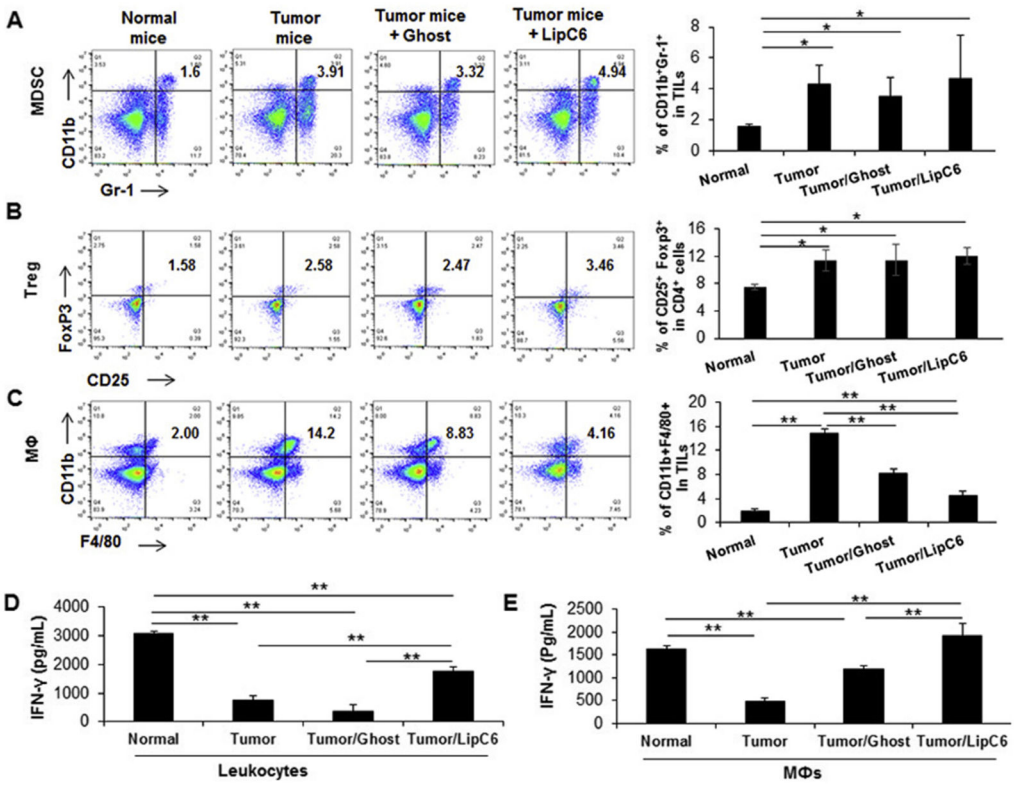

Figure 3.

LipC6 injection reduces suppressive function of TAMs. Size-matched TBMs were randomly assigned to 1 of 3 groups and received vehicle, LipC6, or no injection for 2 weeks. Normal mice served as a control. TILs in tumors and liver-resident lymphocytes LRLs) in livers were harvested after liver perfusion and used to perform the following studies. A portion of TILs and liver-resident lymphocytes were labeled with antibodies against CD4, CD25, FoxP3, F4/80, and CD11b, followed by performance of flow cytometry. (*A*) Quantitated Gr-1$^+$CD11b$^+$MDSCs are shown. (*B*) Quantitated CD4$^+$CD25$^+$FoxP3$^+$Tregs in CD4$^+$ T cells are shown. (*C*) Quantitated CD11b$^+$F4/80$^+$MΦs in TILs and liver-resident lymphocytes are shown. (*D*) 1×10^5 TILs were seeded in 96-well plates and cultured for 48 hours in the presence of anti-CD3 (1 μg/mL) and anti-CD28 (1 μg/mL). IFN-γ concentration in the cultured supernatant was measured by ELISA. Quantitative data for IFN-γ production in TILs are shown. (*E*) LipC6 injection results in the reduction of macrophage suppressive function. TILs were prepared from mice as indicated and used to isolate TAMs by plastic adherence. Prepared TILs suspended in tissue culture media were seeded in cell culture plates at a concentration of 1×10^6 cells/cm^2 surface area. Cultures were incubated for 45 minutes at 37°C then washed 3 times with media, the remaining adherent cells that was > 90% CD11b$^+$ and used as macrophages. 3×10^4 macrophages from each mouse with the indicated injection were co-cultured with 1×10^5 responder cells from splenocytes of wild-type C57BL/6 mice by depleting adherent cells with plastic adherence. After stimulation with 1 μg/mL of anti-CD3 antibody and 1 μg/mL of anti-CD28 antibody for 48 hours, IFN-γ level in the culture supernatants was measured by ELISA. n = 3; error bars represent means ± SD. Asterisk represents significant difference ($P < .05$).

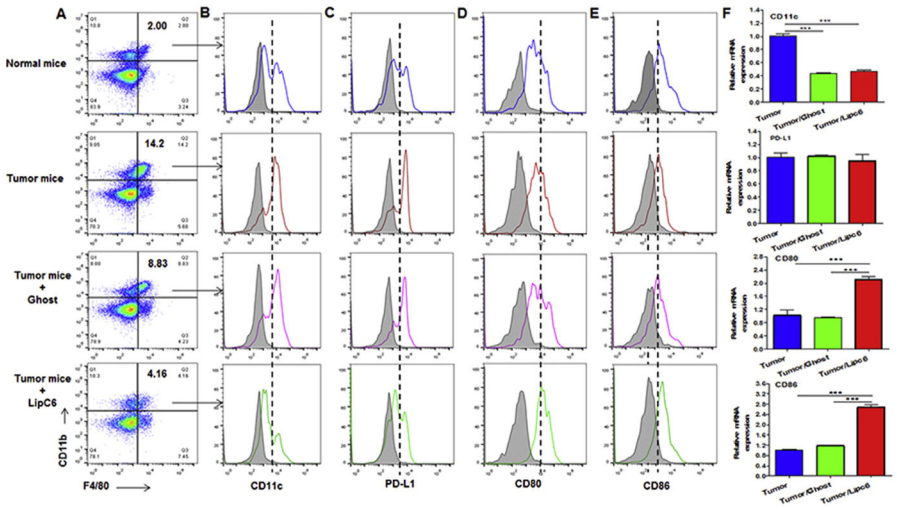

Figure 4.

LipC6 injection blocks up-regulation of M2 macrophage markers. Size-matched TBMs were randomly assigned to 1 of 3 groups: vehicle, LipC6, or no injection. Normal mice served as additional controls. Two weeks after injection, TILs were isolated from the perfused tumors with phosphate-buffered saline and stained with rat IgG isotype control, CD11b, F4/80, CD80, and PD-L1. Flow cytometry was conducted to define the frequency of TAMs positive for both F4/80 and CD11b (*A*). In gated $F4/80^{+}CD11b^{+}$TAMs, the expression of CD11c (*B*), PD-L1 (*C*), CD80 (*D*), and CD86 (*E*) was determined. Part of TILs were also used to isolate TAMs with anti-F4/80 MicroBeads. The total RNAs in the isolated TAMs were extracted and used to conduct real-time PCR for detecting the mRNA level of CD11c, PD-L1, CD80, and CD86 (*F*).

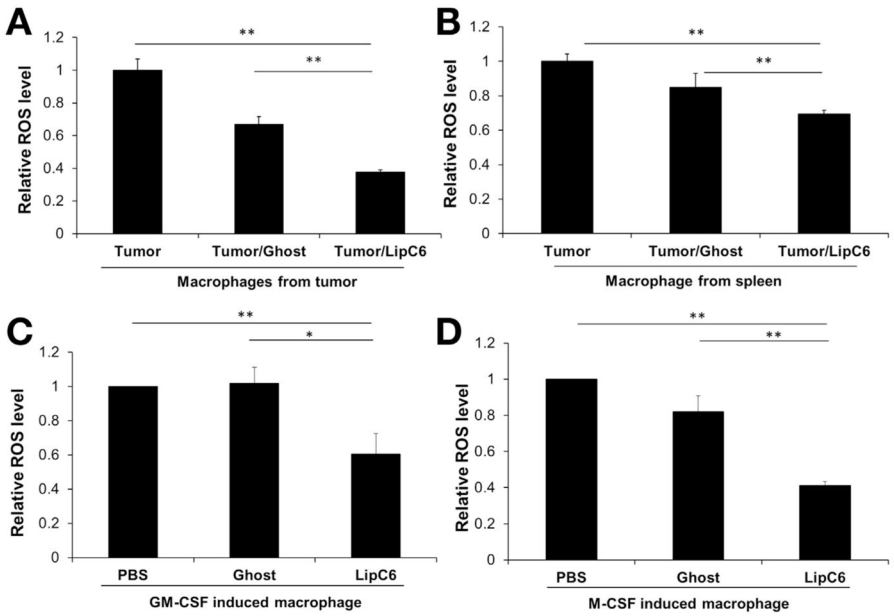

Figure 5.

LipC6 administration suppresses O^{2-} generation in TAMs and BMMs. Size-matched TBMs were randomly assigned to 1 of 3 groups: vehicle, LipC6, or no injection. Two weeks after injection, splenic leukocytes and TILs were prepared from the spleen and the perfused tumors. The cells were incubated for 45 minutes at 37°C, then washed 3 times with media, with the remaining adherent cells being > 90% CD11b positive (macrophages). Intracellular ROS were measured with Glo H_2O_2 assay. Briefly, H_2O_2 substrate was added to each well followed by addition of ROS-Glo detection solution. After incubation for 20 minutes at room temperature, relative luminescence was measured to assess ROS level in TAMs (*A*) and splenic macrophages (*B*). Similarly, BMMs were prepared in vitro by stimulating bone marrow cells from wild-type C57BL/6 mice with GMCSF (G-BMMs) and MCSF (M-BMMs) for 6 days. After incubation with LipC6 or vehicle overnight, the relative ROS level in G-BMMs (*C*) and M-BMMs (*D*) were measured. n = 3; error bars represent ± SD. **P* < .05, ***P* < .01.

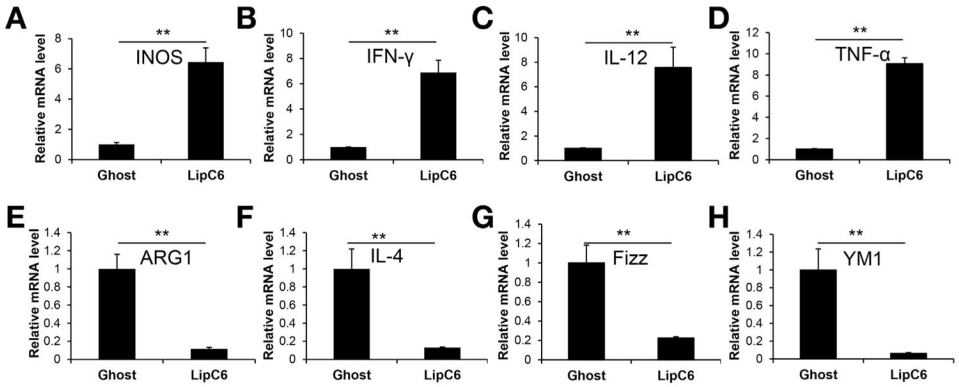

Figure 6.

LipC6 enhances M1 cytokine production and inhibits M2 cytokine production in mouse GMCSF (G-BMMs) and MCSF (M-BMMs). G-BMMs and M-BMMs were prepared in vitro by stimulating bone marrow monocytes from wild-type C57BL/6 mice with GMCSF and MCSF, respectively, for 6 days. The prepared G-BMMs or M-BMMs were subsequently incubated with 25 μmol/L LipC6 or vehicle for 24 hours, the total RNAs are isolated and subjected to real-time PCRs for quantitating enzyme INOS (*A*) and M1 cytokines in G-BMMs including IL12 (*B*), IFN-γ (*C*), TNF-α (*D*); enzyme ARG1 and M2 cytokines in M-BMMs including, IL4 (*E*), FIZZ (*F*) and YM1 (*G*). n = 3; error bars represent ± SD. **P* < .05, ***P* < .01.

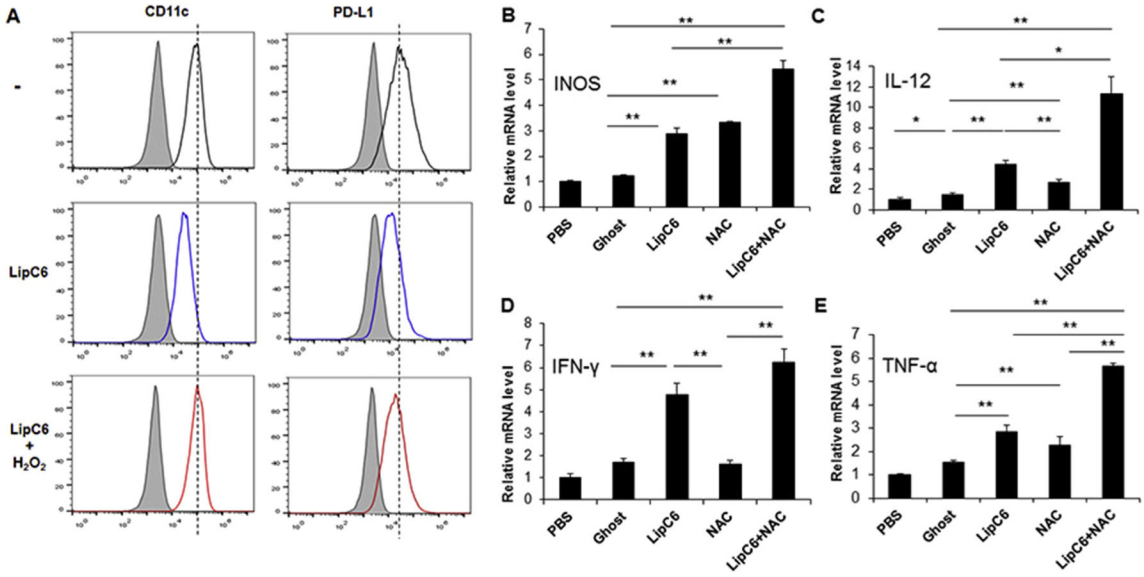

Figure 7.

Impact of LipC6 on phenotype and cytokine production in BMMs. Bone marrow derived monocytes were stimulated with MCSF for 6 hours followed by incubation with LipC6 for 2 hours in the presence or absence of H_2O_2. Cells were subjected to flow cytometry after labeling with antibodies for F4/80, CD11b, CD11c, and PD-1. CD11c or PD-L1–positive cells in the gated $F4/80^+CD11b^+$ macrophage population is shown (*A*). G-BMMs were prepared in vitro by stimulating bone marrow-derived monocytes from wild-type C57BL/6 mice with 50 ng/mL GMCSF for 6 days. GM-BMMs were incubated for 24 hours with 25 μmol/L vehicle, 25 μmol/L LipC6, 50 μmol/L NAC, or LipC6 plus NAC. Total RNA was extracted and subjected to RT-PCR to quantitate M1 cytokines including iNOS (*B*), IL12 (*C*), IFN-γ (*D*), and TNF-α (*E*). n = 3, **P* < .05 and ** *P* < .001 using Student's *t*-test.